

Rapid SAR assessment of electrically thin implantable devices using an analytical approach: Proof-of-Principle for RF heating of coronary stents at 7.0 T

Lukas Winter¹, Eva Oberacker¹, Celal Özerdem¹, Yiyi Ji¹, Florian von Knobelsdorff-Brenkenhoff^{1,2}, Gerd Weidemann³, Frank Seifert³, and Thoralf Niendorf^{1,2}
¹Berlin Ultrahigh Field Facility (B.U.F.F.), Max-Delbrück Center for Molecular Medicine, Berlin, Germany, ²Experimental and Clinical Research Center (ECRC), a joint cooperation between the Charité and the Max-Delbrück Center for Molecular Medicine, Berlin, Germany, ³Physikalisch Technische Bundesanstalt (PTB), Braunschweig and Berlin, Germany

Target audience: Basic researchers and clinical scientists interested in RF safety concepts for small implants, in particular intracoronary stents at ultrahigh fields.

Purpose: En route to broader clinical UHF-MR studies it is essential to gain a better insight into the interaction of passive conducting implants with radiofrequency fields. Early simulation and experimental studies were performed to detail induced SAR levels [1-2]. The conclusions drawn from these studies are valuable but constrained to the very specific experimental setup used. The broad range of patient anatomy, implant position and geometry, RF coil, imaging technique, RF power deposition and RF shimming constitutes an nearly-infinite range of configurations and scattered E-field distributions making SAR assessment challenging if not elusive. Recognizing the need for an universal and rapid approach for SAR assessment of passive conducting implants, this work derives and validates an analytical expression for fast SAR estimation of electrically thin implantable devices. The capabilities of the proposed analytical approach are demonstrated for coronary stents.

Methods: Geometry parameters that effect EM induction in coronary stent configurations commonly used in clinical practice were detailed in EMF simulations (SEMCAD X and CST MWS). Based upon these results, an analytical expression was derived to link $SAR_{1g}(w/o)$ without the presence of a stent with $SAR_{1g}(stent)$ with the presence of a stent. E-field measurements in ASTM like phantoms and RF heating experiments in custom build phantoms were performed to validate the simulation results [3]. To compare the accuracy of the analytical expression, EMF simulations were performed with coronary stents incorporated in human voxel models at different stent positions, for different RF coil configurations and randomly generated phase settings.

Results: Stent length, diameter, orientation and depth dependent SAR induction is displayed in Fig 1. Our simulations confirm the approximation of a stent as an electrically thin element $|k \cdot d/2| \ll 1$ showing that the stent diameter did not influence SAR_{1g} significantly (Fig. 1b). Rotation of the stent by the rotation angle γ away from the E-field vector changes the tangential component of the incident E-field vector E_{tan} responsible for RF induction along the stent (Fig. 1c). An analytical expression is derived in Equ. 1, which links baseline $SAR_{1g}(w/o)$ with $SAR_{1g}(stent)$ via stent specific geometry parameters (Fig. 1g). SAR levels based on the proposed analytical expression (Equ. 1) were benchmarked against human voxel model simulations of a 4-ch loop coil and an 8-ch/16-ch bowtie antenna array. This assessment detected elevated SAR levels for the loop coil in the presence of the stent (Fig. 2). In average the analytical approach overestimated SAR by 14% for the loop coil and by 11%/23% for the 8-/16-ch bow tie antenna array. Our simulation results are supported by E-field and RF heating measurements. The deviation between absolute E-field values w/o stent was -13% and -25% with stent. The deviation between fiber optic thermometry, MR thermometry and thermal simulations was $\Delta T < 1^\circ C$.

$$SAR_{1g}(stent) = [(A \cos(2\gamma) + B) (-0.14x_l^3 + 1.38x_l^2 - 1.7x_l + 2)] \cdot SAR_{1g}(w/o) \quad (1)$$

$$A = -0.035x_l^2 + 0.281x_l - 0.135; \quad A + B = 1;$$

$$1cm \leq x_l \cdot cm \leq 4cm; \quad 0^\circ \leq \gamma \leq 90^\circ$$

Discussion: While covering a broad spectrum of coronary stent configurations, our findings helped to derive an analytical approach which describes SAR_{1g} induced by an arbitrary coronary stent interfering with E-fields generated by an arbitrary RF coil configuration. The analytical estimation can compute induced SAR_{1g} values in real-time allowing detection of SAR levels that exceed the limits given by the IEC guidelines.

Conclusion: Our findings can potentially be translated to any patient, coronary stent type, RF coil configuration and RF transmission regime. Our methodology of a generalized approach, while being backed up by multimodal measurements, may be of value for RF heating investigations of other passive electrically conductive implants even at lower field strengths and provides a novel design criterion for RF coils.

References: [1] Shellock FG, Biomed Res Pub Comp, 2014 [2] Santoro D, et al., PlosONE, 2012 [3] Winter L, et al., MRM, 2014 [4] Christ A, et al., Phys Med Biol, 2010

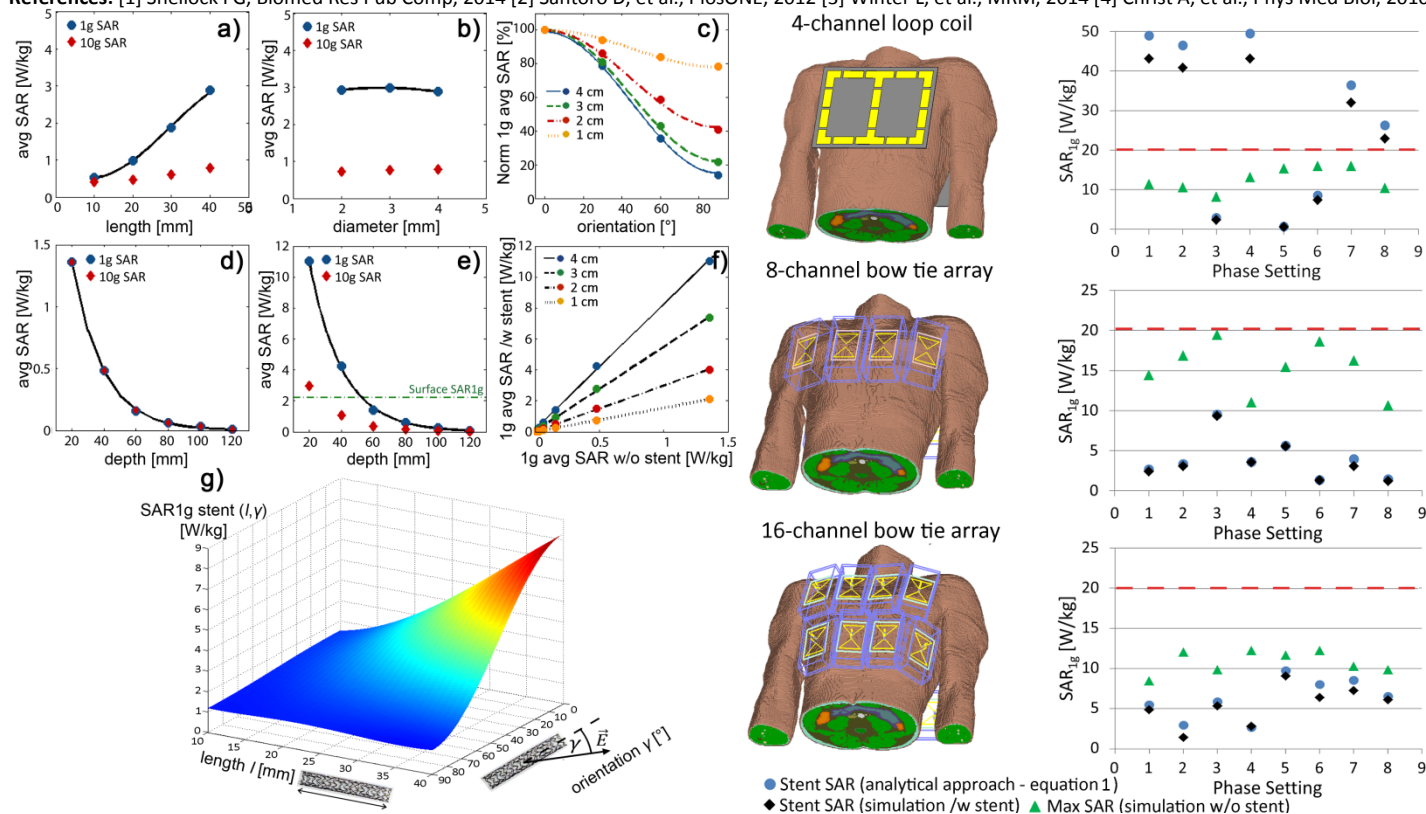


Figure 2 Induced max SAR as a function of a) stent length, b) stent diameter, c) stent orientation and d-f) baseline SAR w/o stent. g) Surface plot of the induced SAR1g values for 1W/kg baseline SAR1g(w/o) utilizing equation 1.

Figure 1 Validation of the real-time SAR prediction using the analytical approach versus stent induced SAR simulations using human voxel model "Duke" [4] for different RF coil array configurations, stent positions and RF phase settings.